Proceedings of the 7th GACM Colloquium on Computational Mechanics for Young Scientists from Academia and Industry October 11-13, 2017 in Stuttgart, Germany

Discussion of crack initiation in metal matrix composites

Markus Sudmanns[1]* and Katrin Schulz[1]

Micro Abstract
Understanding the mechanisms of micro-crack initiation in metals is of high academic as well as industrial interest. In this contribution, we discuss the role of stress concentrations in metal matrix composite materials as the cause of crack initiation. Using a continuum representation of dislocation microstructures, we compare microscale simulations to experimental studies of crack initiation and discuss the dislocation microstructure around a crack tip.

[1]Institute for Applied Materials - Computational Materials Science, Karlsruhe Institute of Technology, Karlsruhe, Germany

* **Corresponding author**: markus.sudmanns@kit.edu

Introduction

Classical approaches to fracture mechanics deal with the propagation of existing cracks. However, a major part of the lifetime regarding material fatigue is spent on micro-crack initiation rather than significant crack propagation [1]. This is also the case in metal matrix composite materials incorporating inclusions, where debonding of the inclusion from the matrix is assumed to take place due to crack initiation at the interface [1]. Therefore the understanding and development of predictive modeling techniques for determining possible locations and causes leading to crack initiation is a central aspect in predicting the failure behavior of a material. In this paper, we discuss the role of stress concentrations in a metal matrix composite as the location and cause of crack initiation. Using a continuum representation of dislocation microstructures, which was previously developed in [2] and the numerical solution method derived in [3], we consider dislocation motion and interaction to determine localizations of concentrated plastic slip in simplified two- and three-dimensional composite systems. We then discuss the influence of resulting stress concentrations regarding crack initiation and subsequent material failure.

Dislocation transport and interaction in a continuum model

The elasto-plastic framework of the formulation used in this paper was introduced in [3] and is based on a decomposition of the distortion tensor into an elastic and a plastic part by $\mathrm{D}\mathbf{u} = \boldsymbol{\beta}^{\mathrm{pl}} + \boldsymbol{\beta}^{\mathrm{el}}$. For the plastic part, we consider only dislocation movement and interaction on multiple slip systems with with the local orthonormal basis $\{\mathbf{d}_s, \mathbf{l}_s, \mathbf{m}_s\}$ and the Burgers vector $\mathbf{b}_s = b_s \mathbf{d}_s$. The evolution of the plastic slip γ_s on each slip systems s is then given by the Orowan equation $\partial_t \gamma_s = v_s b_s \rho_s$ The plastic distortion $\boldsymbol{\beta}^{\mathrm{pl}}$ is given as the summation of the plastic slip over all slip systems $\boldsymbol{\beta}^{\mathrm{pl}} = \sum_{s=1}^{N} \gamma_s \mathbf{d}_s \otimes \mathbf{m}_s$.
Concerning the evolution of the dislocation density ρ_s, we solve a set of partial-differential equations, as introduced in [2]:

$$\begin{aligned}
&\partial_t \rho_s = -\nabla \cdot (v_s \boldsymbol{\kappa}_s^{\perp}) + v_s q_s \qquad \text{with} \qquad \boldsymbol{\kappa}_s^{\perp} = \boldsymbol{\kappa}_s \times \mathbf{m}_s \\
&\partial_t \boldsymbol{\kappa}^s = \nabla \times (\rho_s v_s \mathbf{m}_s) \\
&\partial_t q_s = -\nabla \cdot \Big(\frac{q_s}{\rho_s} \boldsymbol{\kappa}_s^{\perp} v_s + \frac{1}{2|\boldsymbol{\kappa}_s|^2} \Big(\big(\rho_s + |\boldsymbol{\kappa}_s|\big) \boldsymbol{\kappa}_s \otimes \boldsymbol{\kappa}_s - \big(\rho_s - |\boldsymbol{\kappa}_s|\big) \boldsymbol{\kappa}_s^{\perp} \otimes \boldsymbol{\kappa}_s^{\perp} \Big) \nabla v_s \Big)
\end{aligned} \tag{1}$$

To close the equations, we define a velocity law for which we assume a linear dependency on the resolved shear stress τ_{rss} by

$$v_s = v_s(\tau_{rss}) = \frac{b_s}{B}(\tau_{ext} + \tau_{int}) \tag{2}$$

with B as a drag coefficient. τ_{ext} is the projection of the external load on the local slip systems by $\tau_s = \mathbf{d}_s \cdot \boldsymbol{\sigma} \mathbf{m}_s$ and τ_{int} includes the internal stress fields resulting from dislocation interaction. The long-range stresses are resolved by a mean-field approach between different elements. To account for short-range stresses, we add further stress terms based on the formulations described in [4]. To consider interactions of dislocations on different slip systems, we incorporate the extended 'Taylor formulation' developed by [5]

$$\tau_{\mathrm{fl},s} = \mu b_s \sqrt{\sum_j a_{s,j} \rho_j} \tag{3}$$

where μ denotes the shear modulus. This formulation combines the contribution of the density on each slip system ρ_j weighted by the respective interaction strengths $a_{s,j}$ to an average flow stress for each slip system separately.
In the following we will show 2D as well as 3D results. For the 2D case, we simplify the formulation according to [6]. Here we only consider straight edge dislocations in single-slip condition and replace the flow-stress by a model allowing for dislocation dipole interaction, cf. [6].

System setup

We analyze a simplified Al-SiC composite structure. The system geometry is shown in Fig.

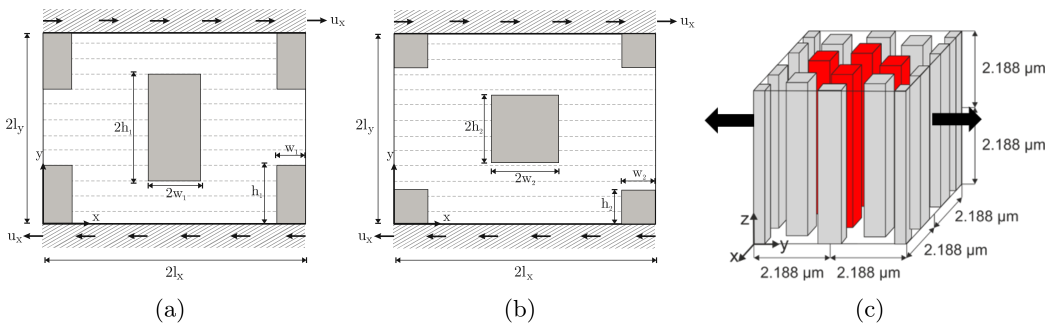

Figure 1. System setup 2D (a,b), cf. [6], and 3D (c) acc. to [7].

1(a,b). It consists of 5 inclusions arranged in hexagonal shape with periodic boundary conditions at the left and right boundaries. We consider two different shapes of the inclusions, one with rectangular inclusions and no unblocked slip planes, see Fig. 1(a) and one with quadratic inclusions, which lead to unblocked slip channels above and below the central inclusion, see Fig. 1(b). The system is rectangular with dimensions $l_y = 2$ μm and $l_x/l_y = \sqrt{3}$. The upper and lower boundaries are subjected to a quasi-static shear loading. The material parameters are given by the elastic moduli $E_{\mathrm{matrix}} = 70$ GPa, $E_{\mathrm{SiC}} = 6.4 \cdot E_{\mathrm{matrix}}$, the Poisson's ratio $\nu_{\mathrm{matrix}} = 0.3$, $\nu_{\mathrm{SiC}} = 0.5 \cdot \nu_{\mathrm{matrix}}$ and a Burger's vector of $b = 0.256$ nm. An initial dislocation density of $\rho = 1.083 \cdot 10^{14} m^{-2}$ is homogeneously distributed over the system. For further details of the model and initial condition is referred to [6].
In a second consideration, we analyze a 3D system, which is shown in Fig. 1 (c). In order to compare the continuum results with Discrete Dislocation Dynamics (DDD) - results from [7], the inclusion distribution and distance has been chosen accordingly. In order to mimic periodic boundaries, we chose a system size of $4.376 \times 4.376 \times 4.376$ μm which is significantly larger compared to [7]. The inclusions have volume fractions of 5, 20 and 45%. The elastic parameters are $E_{\mathrm{matrix}} = 71.3$ GPa, $E_{\mathrm{SiC}} = 5.2 \cdot E_{\mathrm{matrix}}$, $\nu_{\mathrm{matrix}} = 0.347$, $\nu_{\mathrm{SiC}} = 0.67 \cdot \nu_{\mathrm{matrix}}$ and a Burger's

vector of $b = 0.256$ nm. We include all 12 fcc slip systems, the [001]-direction coinciding with the z-coordinate parallel to the vertical axis of the inclusions. The system is initially filled with a homogeneous density of $\rho = 1.75 \cdot 10^{13} m^{-2}$ and then subjected to a transversal tension in y-direction with a constant strain rate of $1000 s^{-1}$.

Results

Using the 2D system shown in Fig. 1(a,b), the stress-strain curves are computed and compared to DDD-data from [8], see Fig. 2(a). It can be seen that blocking all slip planes induces linear hardening, whereas the system with free slip channels shows almost perfect plasticity. The reason for this behavior is that there are strong pile-ups near the interfaces to the inclusions for the system with fully blocked slip planes, see Fig. 2(b, left). In this area, there is high dislocation activity due to stress concentrations induced by inclusion corners. Compared to that, the system with free slip channels shows only very small pile-ups in magnitude and distribution, see Fig. 2(b, right). Here, the plastic slip concentrates almost exclusively on the free slip channels.

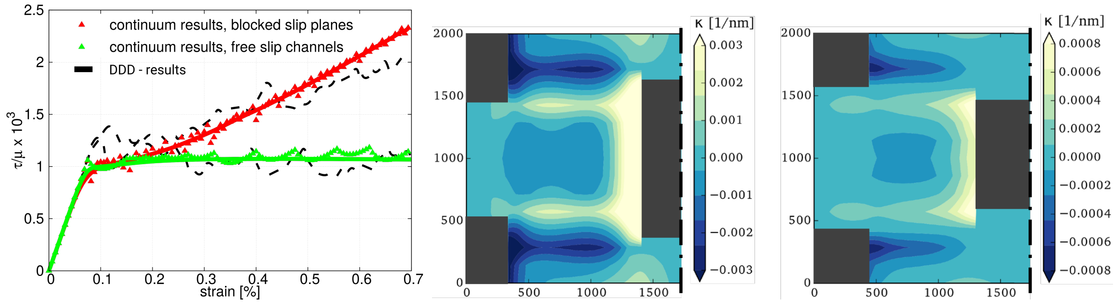

(a) (b)

Figure 2. stress-strain curves compared to DDD-data from [8] (a), pile-ups at inclusions visible in the GND-density distribution for the system with blocked slip planes (b, left) and free slip channels (b, right). For symmetry reasons, only half of the system is shown, cf. also [6].

For the 3D system depicted in Fig. 1(c), the situation is much more complex, since in 3D there are no completely blocked paths available any more. Here, dislocations can move around inclusions, which can be described by the Orowan mechanism. This results in a hardening behavior, which is mainly controlled by the free space between inclusions. Fig. 3(a) shows the stress-strain curves for different inclusion volume fractions compared to DDD-results from [7]. It can be seen that although the yield point is not exactly comparable, which is supposedly due to the different initial configurations of density in DDD and the continuum simulation, the increase in hardening due to a smaller distance between inclusions can be reproduced by the continuum simulation. Fig. 3(b) shows the plastic slip in the system with 20% volume

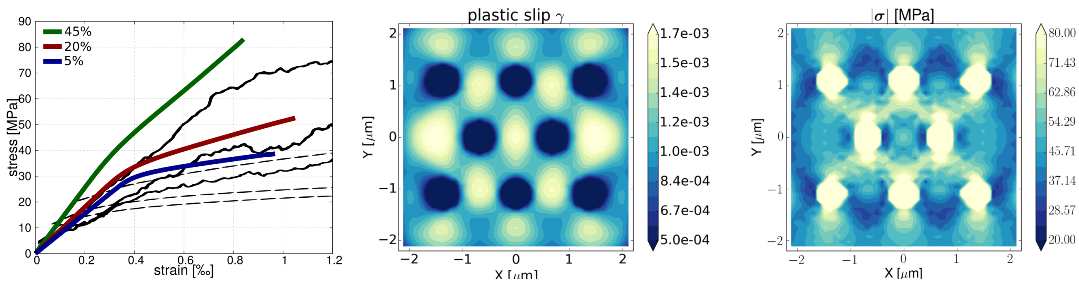

(a) (b) (c)

Figure 3. stress-strain curves for inclusion volume fractions of 5, 20 and 45 % compared with DDD-data from [7] (a), contourplot of the plastic slip distribution summarized over all slip systems for 20% vol. fraction (b) and stress distribution showing stress concentrations at and between inclusions for 20% vol. fraction (c).

fraction plotted normal to the z-axis and summarized over all 12 slip systems. It can be seen that most dislocation activity takes place in unblocked areas. The inhibition of plastic slip between inclusions resulting in a strongly inhomogeneous plastic slip distribution is to some extent induced by an inhomogeneous elastic stress in the matrix due to transversal loading, but also due to back-stress effects induced by pile-ups. Thus a higher stress is needed to push dislocations through the closing channels. This means that the system cannot fully relax the external load in those areas, which then results in higher stresses, see Fig. 3(c).

Discussion and Conclusions

The material behavior of simplified Al-SiC composite structures have been analyzed in 2D and 3D concerning localized plastic slip and stress concentrations. Comparisons with respective DDD-results show good agreement and demonstrates, that the continuum simulation is able to capture key effects observed in discrete simulations. In the 2D system localized plastic slip due to stress concentrations at inclusion corners have been observed. This indicates high dislocation activity and therefore high induced stresses by dislocation pile-ups which yields critical regions concerning failure in metal matrix composites. In the 3D system, the spacing between inclusions has been identified as the key influence to hardening. Here, the inhibition of plastic slip due to the narrow channels results in strong stress gradients inducing critical areas for material failure.

Acknowledgements

The financial support for the research group FOR1650 *Dislocation based Plasticity* funded by the German Research Foundation (DFG) under the contract number GU367/36-2 as well as the support by the European Social Fund and the state Baden-Wuerttemberg is gratefully acknowledged.

References

[1] K. Tanaka and T. Mura. A theory of fatigue crack initiation at inclusions. *Metallurgical Transactions A*, 13(1):117–123, Jan 1982.

[2] Thomas Hochrainer, Stefan Sandfeld, Michael Zaiser, and Peter Gumbsch. Continuum dislocation dynamics: Towards a physical theory of crystal plasticity. *Journal of the Mechanics and Physics of Solids*, 63:167 – 178, 2014.

[3] Katrin Schulz, Lydia Wagner, and Christian Wieners. A mesoscale approach for dislocation density motion using a runge-kutta discontinuous galerkin method. *PAMM*, 16(1):403–404, 2016.

[4] S. Schmitt, P. Gumbsch, and K. Schulz. Internal stresses in a homogenized representation of dislocation microstructures. *Journal of the Mechanics and Physics of Solids*, 84:528–544, 2015. cited By 3.

[5] A. Zaoui Franciosi P, M. Berveiller. Latent hardening in copper and aluminium single crystals. *Acta Metallurgica*, 1980.

[6] Katrin Schulz, Markus Sudmanns, and Peter Gumbsch. Dislocation-density based description of the deformation of a composite material. *Modelling and Simulation in Materials Science and Engineering*, 2017.

[7] S. Groh, B. Devincre, L.P. Kubin, A. Roos, F. Feyel, and J.-L. Chaboche. Size effects in metal matrix composites. *Materials Science and Engineering: A*, 400–401:279 – 282, 2005. Dislocations 2004An International Conference on the Fundamentals of Plastic Deformation.

[8] S. Yefimov, I. Groma, and E. van der Giessen. A comparison of a statistical-mechanics based plasticity model with discrete dislocation plasticity calculations. *Journal of the Mechanics and Physics of Solids*, 52(2):279 – 300, 2004.